ACS OMEGA

http://pubs.acs.org/journal/acsodf

Article

Tungsten Disulfide Decorated Screen-Printed Electrodes for Sensing of Glycated Hemoglobin

Sunil Kumar Mahobiya, Sapna Balayan, Nidhi Chauhan, Manika Khanuja, Naresh K. Kuchhal, S. S. Islam, and Utkarsh Jain*

Cite This: *ACS Omega* 2022, 7, 34676−34684

Read Online

ACCESS | Metrics & More | Article Recommendations

ABSTRACT: Diabetes is a global menace, and its severity results in various disorders including cardiovascular, retinopathy, neuropathy, and nephropathy. Recently, diabetic conditions are diagnosed through the level of glycated hemoglobin. The level of glycated hemoglobin is determined with enzymatic methodology. Although the system is sensitive, it has various restrictions such as long processing times, expensive equipment required for testing, and complex steps involved in sample preparation. These limitations are a hindrance to faster results. The limitations of the developed methods can be eliminated through biosensors. In this work, an electrochemical platform was fabricated that facilitates the identification of glycated hemoglobin protein in diabetic patients. The working electrode on the integrated circuit was modified with molecularly imprinted polymer decorated with tungsten disulfide nanoparticles to enhance its analytical properties. The analytical properties of the biosensor were studied using electrochemical techniques. The obtained detection limit of the nanoelectronic sensor was 0.01 pM. The calculated sensitivity of the biosensor was observed to be 0.27 μA/pM. Also, the sensor promises to operate in a dynamic working concentration range and provide instant results.

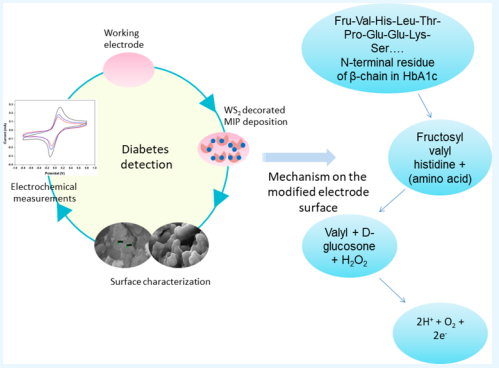

1. INTRODUCTION

Diabetes was introduced in ancient scripts, and it has been considered as a serious illness. However, its effect was not studied by the healers or physicians of the past. In the last few decades, it has been observed that human health and development are continuously affected by the increasing cases of diabetic conditions. Major health issues are observed due to the changes in the living standards of human beings. The changing lifestyle, unhealthy diet, and reduced exercise have all resulted in an epidemic disease called diabetes mellitus (DM). This is a chronic health condition that affects the energy produced in the body through food taken.[1−3] Diabetes is a challenging and growing healthcare condition worldwide. It is a metabolic disease that is caused due to the deficiency of insulin or its secretion. The increased level of blood sugar has a lasting impact on the patient's body, with some of these effects being organ failure (eyes, blood vessels, nerves, kidneys, and heart) or dysfunction. The latest reports generated by the International Federation of Clinical Chemistry and Laboratory Medicine (IFCC) show that about 415 million people are affected by diabetes globally, and 47% of the population are not aware of their condition.[4−7] Globally, it was observed that the number of adults suffering from diabetes increased from 198 (1980) to 422 (2014) million. The global prevalence increased from 4.7 to 8.5% in 1980. Over the past decade, the rate of diabetic patients is rising at a faster speed in developing countries rather than in developed countries. In 2012, about 1 million deaths were reported due to diabetes. Another 22 million deaths were recorded due to cardiovascular and other diseases that occurred because of higher-than-optimal blood glucose.[8]

Types of diabetes can lead to complications in different parts of the human body, and there is a higher risk of premature death. Complications that can occur due to diabetes are vision loss, stroke, heart attack, nerve damage, leg amputation, and kidney failure. During pregnancy, diabetes can result in various complications and also the risk of fetal death. The diabetic condition is usually developed due to the aging factor or obesity. In consideration with the American Diabetes Association, the diabetic condition can be categorized into four classes: syndrome monogenic diabetes, type 1 diabetes (T1D), gestational diabetes mellitus (GDM), and type 2 diabetes (T2D). Type 1 diabetes occurs due to the degradation

Received: August 3, 2022
Accepted: September 1, 2022
Published: September 14, 2022

of insulin which helps in the production of B cells. These B cells are destroyed by the active T cells accidentally. Cases of type 1 diabetes are mainly (95%) caused due to autoimmunity, whereas only 5% of cases are idiopathic.[9] In type 2 diabetes, the use of insulin is not properly carried out by the body. There is a majority of people who are affected by type 2 diabetes. In previous times, the diabetes condition was limited to adults, but at present, it has exceeded among children and infants. The currently available knowledge on type 1 diabetes is not sufficient to prevent it. Recently, various effective approaches are available that help to prevent type 2 diabetes, and this can control premature death and severe complications. Healthy eating, regular exercise, controlling lipids and blood pressure, and avoiding smoking are good practices for controlling diabetes.[8]

The detection of diabetes is becoming an important factor globally. Detection in the early stages can help in the control and management of the condition. Presently, various analytical and electroanalytical approaches have been employed to identify biological and environmental compounds. Analytical methods like high-performance liquid chromatography, thin-layer chromatography, capillary electrophoresis, and spectrophotometry are the popular methods available for determination. Despite various advantages, it has some drawbacks, such as complex sample preparation, time consumption, and special instruments required for the application. The electroanalytical methods can provide various advantages over the analytical methods as they are cost-effective and feasible, provide instant results, have a broad linear range, higher specificity, and better reproducibility, are portable, and have a longer storage period.[10−15]

Recently, different methods can be used for the detection of diabetes such as high-performance liquid chromatography (HPLC), boronate affinity chromatography, thiobarbituric acid (TBA), and ion exchange chromatography.[16−19] Although these methods are producing sensitive results, they also have various drawbacks like expensive instruments and infrastructure, smaller storage periods, and long processing time, with a complex and time-consuming sample preparation process.[20−22] Therefore, new technology and methods are needed to be introduced for removing these constraints, and a promising solution to this problem can be the use of biosensors.[23−26] Therefore, in this study, an electrochemical nanobiosensor was introduced. The biosensor is designed to identify the level of glycated hemoglobin (HbA1c) in diabetic patients. HbA1c is a protein that is present in the form of glycosylation in the body. The level of HbA1c facilitates determining the average blood glucose for a period of 2 to 3 months. It can help in monitoring glucose levels over a long time and also studying potential diabetes risk factors in complicated patients. The level of HbA1c has been set by the World Health Organization (WHO) and American Diabetes Association (ADA). If the cutoff value for HbA1c is ≥6.5%, then the patient is diabetic.[27−31]

Therefore, HbA1c was chosen as the potential protein for diabetes detection. The nanobiosensor is designed on an integrated electronic platform that is a screen-printed electrode (SPE). The size of SPE is in centimeters (i.e., very small); therefore, this nanosensor can be transformed into a miniaturized device that can be used in point-of-care (POC) applications. The surface of the electrode was modified with tungsten disulfide (WS_2) nanoparticles (NPs) decorated on the molecularly imprinted polymer (MIP). The NPs can enhance the properties of a biosensor by increasing the surface area-to-volume ratio (SA/V), electron transfer, and a large surface area.[32,33] MIPs are artificial recognition elements. They provide higher sensitivity, specificity, and thermal stability. MIP integrated biosensing platforms are stable at higher temperatures and pressure.[34−40] In this work, fructosyl amino acid oxidase was used as a template and HbA1c as an analyte. The concentration of HbA1c is determined with further experimentation, and different conditions were examined on the biosensor surface to check and evaluate the activity, stability, and other parameters of the designed nanobiosensor. The MIP-based biosensor promises to show higher stability in comparison with enzyme-based biosensors. The working of the biosensor was recorded in a wide concentration range and provides a lower limit of detection. Also, the sensor shows higher sensitivity.

2. MATERIALS AND METHODS

2.1. Reagents and Apparatus Required. Ethylene glycol dimethacrylate (EGDMA), fructosyl amino acid oxidase (FAO), acetonitrile, and methyl acrylate acid (MAA) were procured from the U.S.A. originated company Sigma-Aldrich. An India-based company, Sisco Research Laboratories Pvt. Ltd. (SRL)-India, provided other reagents such as acetonitrile (ACN), tungsten trioxide (WO_3), sulfur potassium, ferro/ferricyanide, distilled water (DW), and azobis(isobutyronitrile) (AIBN). Screen-printed carbon electrode was purchased from Palmsens, a company in The Netherlands. A potentiostat from Bio-Logic (SP-190) company in France was used to carry out the electrochemical measurements.

2.2. Tungsten Disulfide NP Synthesis. The preparation of WS_2 NPs was carried out with the chemical vapor deposition (CVD) method. For the preparation of WS_2 NP precursors, WO_3 and sulfur (S) were used. The CVD method was carried out at atmospheric pressure for WS_2 NPs. Argon gas was used as a carrier gas during the synthesis. A ceramic boat was used to place the precursor sulfur and WO_3 in a quartz tube containing a hole. This quartz tube was then inserted into the furnace, and the temperature of the furnace was set to 1070 °C while the heating rate of the system was set to 15 °C/min.[41] The placement of the precursor WO_3 was at the center of the heating zone of the furnace, whereas precursor S was placed outside from the heating center at a distance of 18−20 cm for proper radiation by the emitting heat. The holding time of the furnace was 15 min.

2.3. Molecularly Imprinted Polymer for FAO. A molecularly imprinted polymer is a three-dimensional matrix. The synthesized MIP is highly specific to the FAO molecule. The preparation of molecularly imprinted polymer for FAO was completed using bulk polymerization. The reagents such as MMA, EGDMA, and FAO were immersed in a porogen ACN (50 mL) and WS_2 NPs within a specific ratio. The mixture was sonicated for 30 min to form the homogeneous solution, and then nitrogen gas was passed through the solution for 15 min for oxygen removal. Further, the mixture was stirred at a temperature of 45 °C for 15 min. The initiator AIBN was added, and inert conditions were maintained so that the polymerization process can occur; the mixture was kept for 48 h under this condition. The resultant MIP was a white powder, and this white powder was then crushed and dried properly for experimentation and characterization.[6,7,19−21] Scanning electron microscopy was used to observe the surface of MIP with the FAO molecule.

https://doi.org/10.1021/acsomega.2c04926
ACS Omega 2022, 7, 34676−34684

Scheme 1. Pictorial Representation of Steps Involved in Designing the Nanobiosensor for HbA1c Detection

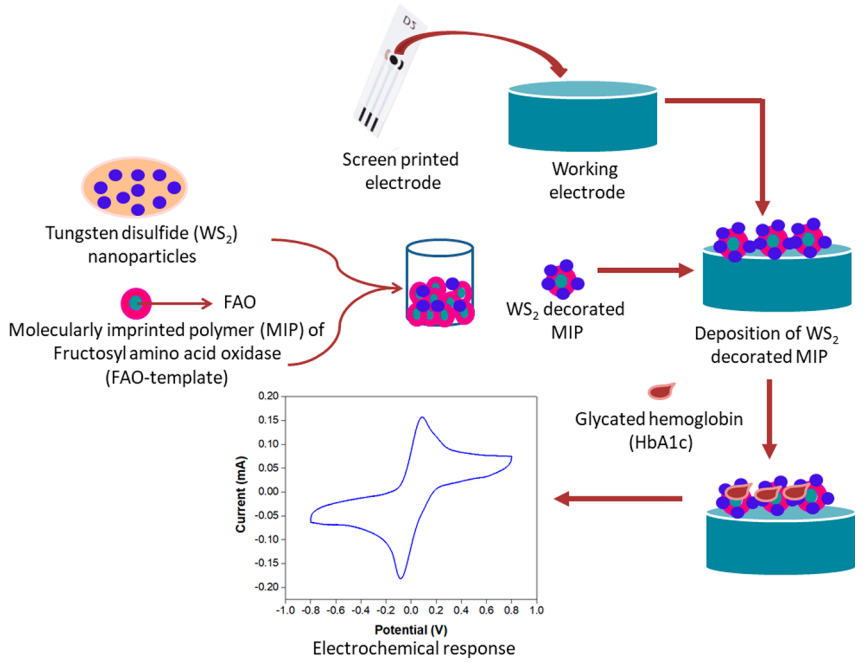

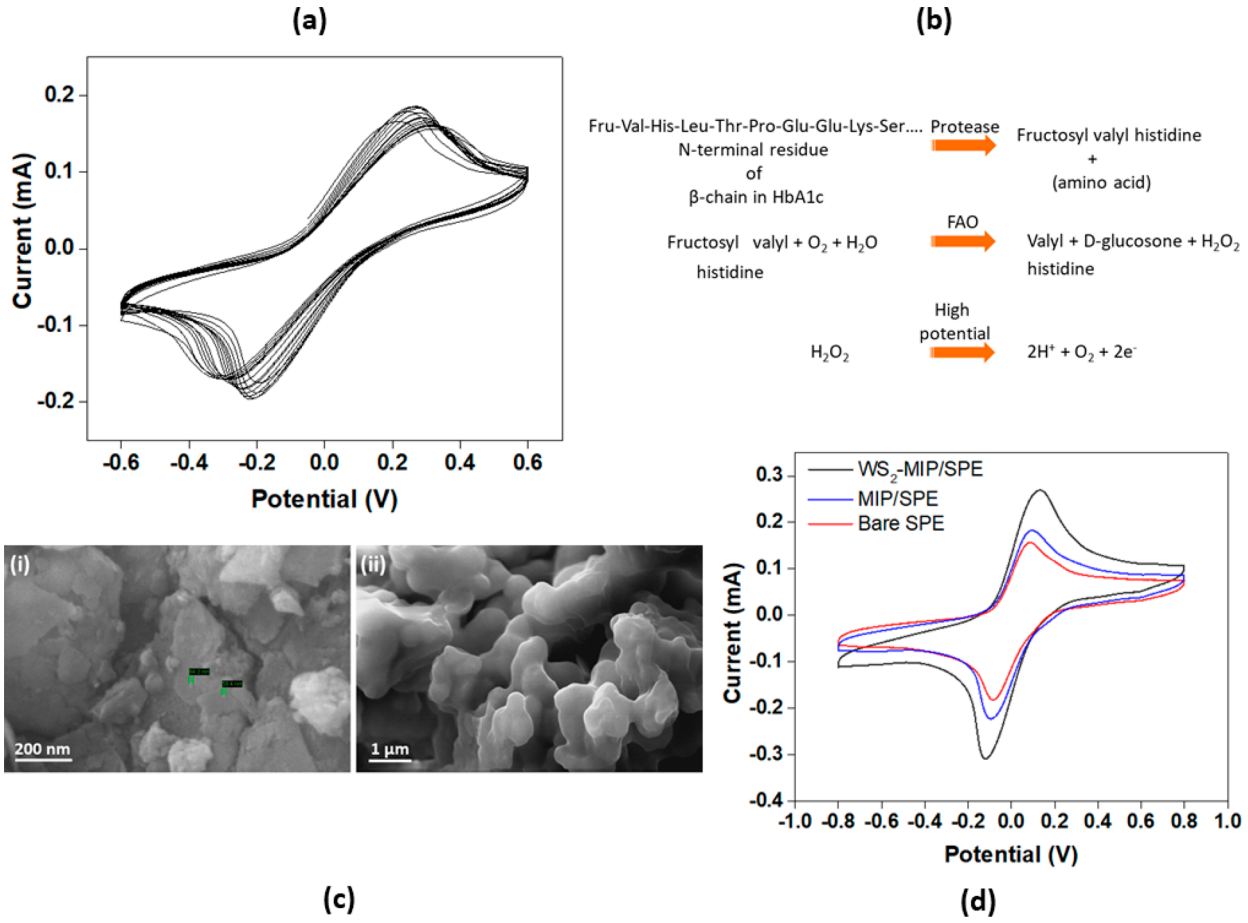

Figure 1. Surface modification of screen printed electrode. (a) Electrodeposition of WS_2-MIP on SPE with cyclic voltammetry (in 5 mM electrolyte solution, scan rate 50 mV/s, and potential −0.6 to 0.6 V for 15 cycles). (b) Mechanism occurring on the surface of the modified electrode. (c) Scanning electron microscopy for surface characterization of (i) WS_2 nanoparticles and (ii) molecularly imprinted polymer for FAO. (d) Electrochemistry curve for developed nanobiosensor at each stage: (i) bare SPE (red); (ii) MIP (control, blue); (iii) WS_2-MIP (black) on electrode surface.

https://doi.org/10.1021/acsomega.2c04926
ACS Omega 2022, 7, 34676−34684

2.4. Stepwise Development of Sensing Platform. *2.4.1. Electromodification of SPE with Synthesized Molecularly Imprinted Polymer Decorated with WS_2 NPs.* The stepwise development of the biosensor is displayed in Scheme 1. The modification on the electrode was done with WS_2 decorated MIP. The deposition was carried out with an electrochemical technique. Here, cyclic voltammetry (CV) was used for deposition, and the potential window was considered from −0.6 to +0.6 V for 15 cycles. Figure 1a displays the CV cycles for deposition of WS_2-MIP on the SPE surface. The *x*-axis in the graph represents the potential window during the deposition process, and the *y*-axis shows the current value on each deposition. The electrodeposition was carried out in the presence of a ferro/ferrielectrolyte solution of 5 mM and 7 pH. Also, a control experiment was performed with the synthesized MIP in the absence of WS_2 NPs. After, coating the surface area of the electrode was calculated in both cases (unmodified and modified electrode). It was observed that the surface area of the unmodified electrode was 2.14 mm^2, and the surface area of the modified electrode was 2.7 mm^2.

2.4.2. Electrochemical Study of a Modified Electrode Surface. The activity of the developed nanobiosensor was examined using electrochemical techniques on the potentiostat manufactured by a France-based company BioLogic (SP-190). In this work, CV, differential pulse voltammetry (DPV), and square wave voltammetry (SWV) were applied to record the activity of the reformed electrode. The modification stages of the electrode were studied with CV. The response of the electrode was obtained with the varying concentration of HbA1c. Further, the electrode was evaluated with varying pH and temperature. A scan rate study was carried out for examining the kinetics of the system. The selectivity of the biosensor was determined by various interfering compounds (uric acid, acetylcholine, cholesterol, and glucose). The repeatability of the data was checked with seven electrodes that were prepared at similar conditions.

2.5. Working on the Developed Biosensor. The present study is based on the development of a biosensor with the integration of MIP for FAO. The surface of the working electrode was modified with WS_2 NP decorated MIP. The NPs enhance the analytical properties of the electrode with increased surface area and higher electron mobility that lead to enhanced conductivity and surface-to-volume ratio. The molecules of FAO bind with HbA1c, and the electrons are generated which were used to interpret the concentration of the analyte. A control experiment was performed with only MIP in the absence of NPs to check the value of oxidation and reduction peaks.

2.5.1. Mechanism for the Developed Biosensor. The blood samples were treated with ethylenediamine tetraacetic acid (EDTA) which was used as an anticoagulant. The whole blood was mixed with lysis buffer to obtain the hemolysis. The proteolytic digestion of the blood samples was carried out in the presence of purified 4U/mL *Bacillus* spp. proteases, 1 mM oxidizing agent, and 5 mM of 4-morpholinoethane sulfonic acid. The performed proteolytic digestion resulted in the release of amino acids, and this also included glycated valines that are released from the beta chains of hemoglobin. The glycated valines now serve as a substrate for the FAO enzyme which continuously produces H_2O_2. This results in the breaking of N-terminal amino acids. The electrons generated during this process are measured in the term of current. The principle of detection is based on the H_2O_2 splitting occurring due to the FAO oxidation. The splitting of H_2O_2 is directly proportional to the concentration of HbA1c.[42] The mechanism of this process is shown in Figure 1b.

3. RESULTS AND DISCUSSION

3.1. Characterization of Prepared NPs and MIP. The WS_2 synthesized NPs were characterized with scanning electron microscopy (SEM). As shown in Figure 1c(i), the sphere-like shapes visible on the surface corroborate the synthesis of WS_2 NPs. The size of the nanomaterial was determined to be within a range from 58.4 to 64.3 nm. These nanoparticles provide a higher SA/V. The nanomaterial enhances the electron transfer and this leads to higher electrical conductivity on the redesigned surface of the integrated circuit (SPE). Thereafter, the synthesized MIP was also characterized by SEM as shown in image (ii) of Figure 1c. In the case of MIP, the SEM images show a similar molecular pattern over the surface. These structures are for FAO molecules. The HbA1c molecules bind to the FAO structures, and chemical activity on the surface was measured with CV. The MIPs are highly specific to the target molecule, and they provide longer stability at higher temperatures and pH.

3.2. Nanoelectrochemistry of a Designed Biosensor at Each Stage. The designed nanobiosensor was examined using an electrochemical technique. Figure 1d describes the CV response of biosensors for different cases. It was observed that the SPE with electron mediator gave lower oxidation and reduction peaks. Here, in this study, in the first step, ferrocyanide and ferricyanide were used as an electron mediator. First, when CV was performed, the oxidation and reduction peaks obtained showed lower current values because no biochemical reaction was occurring on the surface of the electrode. When the electrode was coated with WS_2-MIP, the bioelectrocatalysis process takes place. The enhancement in the oxidation and reduction peaks occurs due to the exchange of electrons on the surface of SPE in the presence of the electron mediator. A potential window from −0.8 to +0.8 V was applied to obtain CV results. Hence, higher charge diffusion takes place on the SPE. The nanomaterials facilitate a higher electron transfer, hence, increasing the conductivity of the biosensor. The control experiment shows that coating of MIP in the absence of WS_2 NPs results in lower oxidation and reduction peaks.

3.3. Response of Biosensor at Varying Concentrations of HbA1c. The varying concentrations of HbA1c were investigated with DPV. Figure 2 describes the DPV curves obtained on the surface of the SPE in the presence of different concentrations. The results were obtained at −0.5 V and with an electron mediator of 5 mM (ferro/ferri) and pH 7. The current value increases simultaneously with the increasing concentration of HbA1c. The lowest current value of approximately 12.9 μA was observed at the smallest concentration (0.01 pM); further, with the increase in the concentration, the current value reaches its maximum at the highest concentration. The interaction of FAO and the HbA1c molecule is greater at higher concentrations; therefore, a large number of electrons are generated, which results in the enhancement of the current on the working electrode. The working concentration range of the biosensor was calculated from 0.01 pM to 100 mM, and the sensitivity was 0.27 μA/pM. Also, the biosensor shows a very lower limit of detection at 0.01 pM.

https://doi.org/10.1021/acsomega.2c04926
ACS Omega 2022, 7, 34676−34684

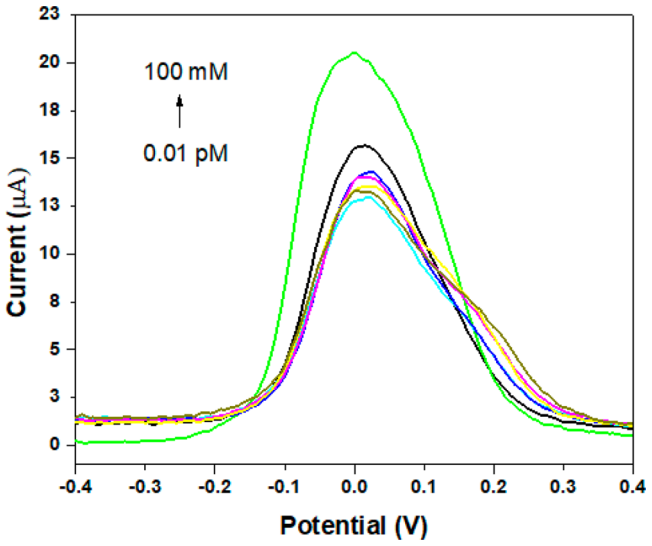

Figure 2. Differential pulse voltammetry studies for HbA1c concentrations from 0.01 pM to 100 mM in the presence of ferro/ferrielectrolyte of 5 mM and pH 7 at a potential of −0.5 V.

3.4. Optimized Parameters for the Fabricated Nanobiosensor. *3.4.1. Deposition Cycle for MIP on the SPE Surface.* The deposition of WS_2 decorated MIP was carried out with CV, and the potential range for deposition was chosen to be from −0.6 V to +0.6 V. The deposition was carried out in the presence of a 5 mM (7 pH) electron mediator of 20 μL and WS_2-MIP solution of 80 μL. The optimization study was carried out with a different number of deposition cycles, that is, 5, 10, 15, and 20. The DPV curves were obtained for various observations. In the first case, 5 CV cycles were run for deposition. Thereafter, the sample was removed from the electrode surface, and washing was done to remove unbounded reactants; the electrode was then dried. Now, in the presence of ferro/ferri, DPV results were obtained to study the deposition cycle of WS_2-MIP on the electrode surface. The DPV results were obtained at a potential of −0.5 V. Similarly, the same steps were carried out for all four cases, and the maximum value of current among the four cases was obtained after 15 cycle depositions (that is case 3), as shown in Figure 3a (error bar represents ±2 standard error (SE)). After 15 cycles, the peak current started to decrease. Therefore, 15 cycles were used for depositing the WS_2-MIP on the electronic platform.

3.4.2. Incubation Time of the Developed Nanosensor. Incubation time is an important factor in the evaluation of a biosensor. It helps to study the interaction between the FAO and HbA1c molecules. The activity of the working electrode was checked at different incubation times ranging from 5 to 25 min, and the interval was 5 min (5, 10, 15, 20, 25). The DPV measurements were carried out at −0.5 V with ferro/ferri solution (5 mM; pH 7). It was observed that the peak current rises from 5 to 10 min, and after 10 min incubation, the peak current starts decreasing. Therefore, it can be concluded that the interaction between FAO and HbA1c reaches a balance after 10 min. A bar graph demonstrates the difference in the peak current for distinct cases, as shown in Figure 3b (error bar represents ±2 SE). The figure represents the peak value of DPV analysis with different incubation times. Hence, the incubation time for the designed biosensor was selected as 10 min.

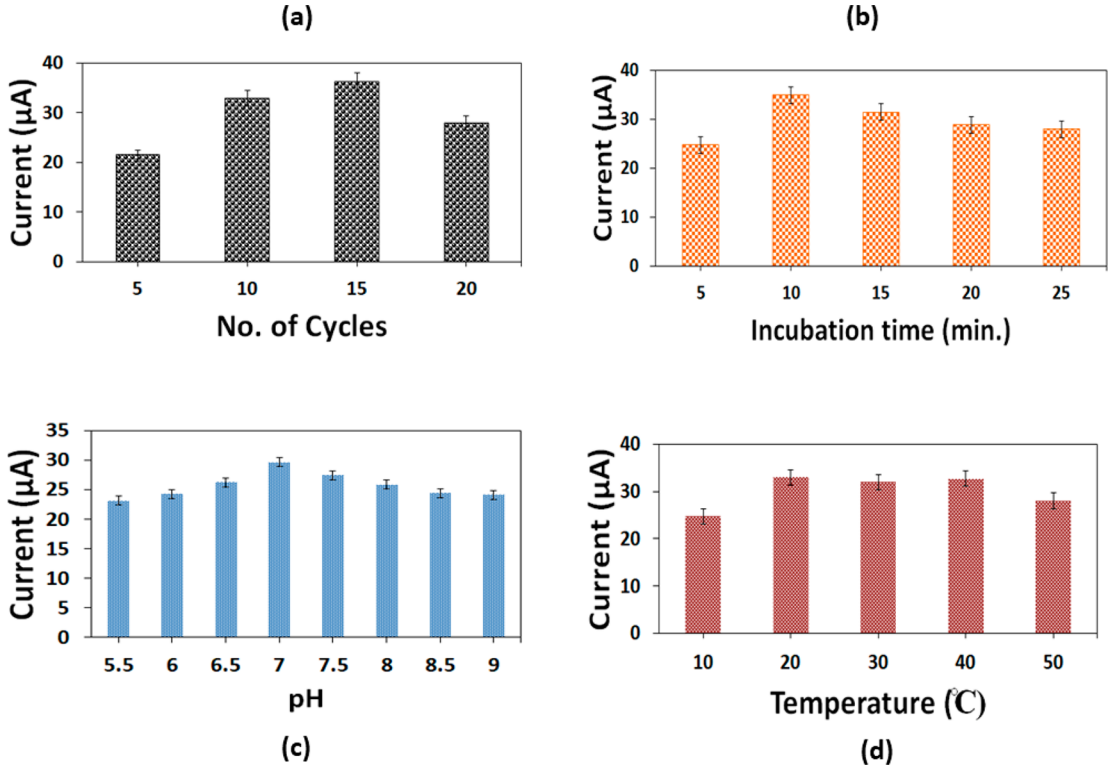

Figure 3. Optimization studies: (a) MIP deposition cycle (5−20 with an interval of 5 cycles); (b) incubation time (5 to 25 min interval of 5 min); (c) pH 5.5 to 9 with the difference of 0.5 units; (d) temperature (10 to 50 °C, with an interval of 10 units); all the measurements were carried out in the presence of ferro/ferri electron mediator (5 mM; pH 7).

https://doi.org/10.1021/acsomega.2c04926
ACS Omega 2022, 7, 34676−34684

3.4.3. pH and Thermal Stability of the Assembled Biosensor. The designed biosensor was evaluated with different pH solutions. The pH of the solution highly influences the binding of FAO and MIP. The effect of pH on the activity of the biosensor was evaluated from pH 5.5 to 9. The pH response of the electrode was determined with DPV measurement. The peak value obtained with the DPV study is represented in the bar graph in Figure 3c (the error bar represents ±2 SE). The potential was applied at −0.5 V for DPV measurements. It can be observed that the peak current rises from pH 5.5 and is maximum at pH 7. This shows that the electrode operates best in a neutral atmosphere; therefore, pH 7 was considered to be the optimum pH for the constructed biosensor.

Further, the thermal stability of the designed SPE was studied with varying temperatures from 10 to 50 °C with intervals of 10 °C chosen for analysis. The DPV analysis was carried out in the presence of a ferro/ferri mediator, and the applied voltage was −0.5 V. The peak value obtained at different temperatures is displayed using the bar graph in Figure 3d (the error bar represents ±2 SE). The maximum electrode current was obtained at 20 °C. Therefore, it was selected as the optimized temperature for the fabricated biosensor.

3.5. Cyclic Voltammetry at a Different Scan Rates for Biosensor Stability. The electrochemical reaction rate of the target molecule was examined using the scan rate study. For the scan rate study, CV results were obtained in the voltage range from −1.0 V to +1.0 V for the designed SPE. All of these measurements were carried out in the presence of ferro/ferri (5 mM; pH 7). The scan rate range was selected from 20 to 140 mV/s. Figure 4a represents the CV curves for different scan rates. The observation made depicts that there is an increase in the oxidation and reduction peaks with the simultaneous increase in the scan rate. For studying the electron-transfer kinetics, a graph was plotted considering the peak value of oxidation and reduction versus scan rate, as shown in Figure 4b. The graph plotted represents the linearity for both cases (oxidation and reduction) with the increasing scan rate.

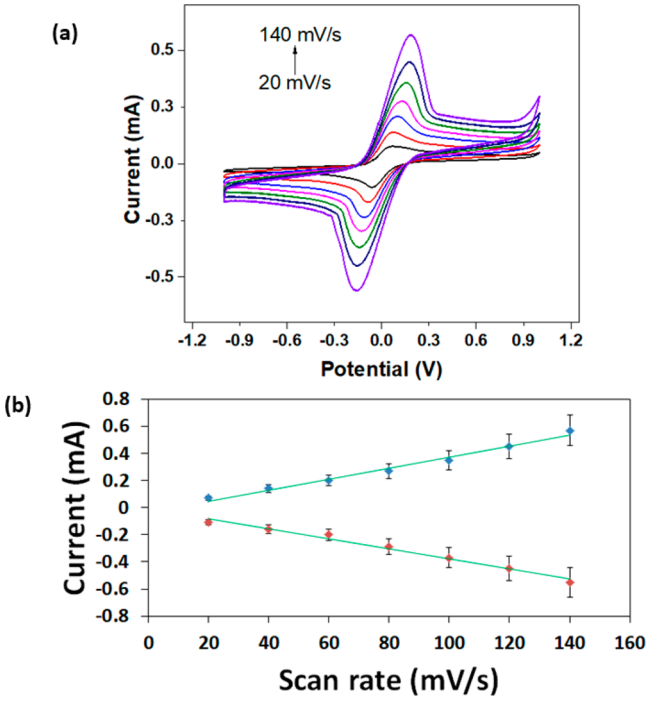

Figure 4. Scan rate studies: (a) cyclic voltammetry at different scan rates from 20 to 140 mV/s; (b) linear graph with oxidation and reduction peak at different scan rates.

3.6. Activity of Modified SPE with Various Interfering Compounds. There are various interfering compounds available in real blood samples. Therefore, the developed biosensor was evaluated with all of the possible interferences that can affect the activity of the biosensor. The included interfering compounds in the work are acetylcholine, ascorbic acid, cholesterol, glucose, and uric acid.[43] DPV measurements were used to record the result at −0.5 V. The experimentation was carried out in the presence of an electrolyte (5 mM and pH 7). The activity loss of the biosensor was calculated, and the loss was observed between 10 and 15%. For each interfering compound, the activity loss was 5.1% for acetylcholine, 11.3% for ascorbic acid, 4.7% for cholesterol, 1.4% for glucose, and 2.0% for uric acid. The activity loss of the biosensor is shown in Figure 5a (the error bar represents ±2 SE).

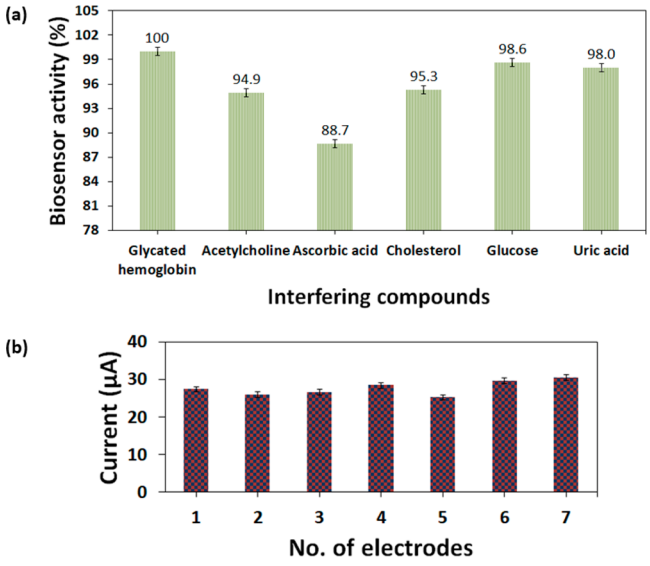

Figure 5. (a) Interference studies with different compounds (5.1% acetylcholine, 11.3% ascorbic acid, 4.7% cholesterol, 1.4% glucose, 2.0% uric acid). (b) Repeatability data for developed nanobiosensor with electrodes prepared similarly.

3.7. Checking the Stability and Repeatability of the Designed Nanobiosensor. Stability is an important parameter for any biosensor. In this work, the stability of the biosensor was determined by conserving the designed electrode for 2 months. The activity of the nanosensor was checked every 10 days. It was noted that after a period (6 weeks), the activity of the biosensor starts decreasing and a 20% loss was obtained in the biosensor activity. The 20% activity loss after 6 weeks for the fabricated biosensor is considerable. The storage of the electrode was done properly in a dry place, and the temperature was maintained at 4 °C. The repeatability of data for the fabricated nanobiosensor was checked with seven electrodes that were prepared at the same time, and all of the conditions were kept similar. Figure 5b (error bar represents ±2 SE) shows the data for electrode

https://doi.org/10.1021/acsomega.2c04926
ACS Omega 2022, 7, 34676−34684

Table 1. Comparison of Results of Constructed Biosensor and Platforms Reported in the Literature

S.no.	Platform	Limit of detection	Detection range	Incubation time	Sensitivity	Ref
1	Aptasensor	2.8 nM	100 pg/mL to 10 μg/mL	30 min	0.2 ng/mL	44
2	Aptasensor	1 nM	18−147 nM	1 h	N/A	45
3	Luminol chemiluminescence	350 ng/mL	50−1000 μg/mL	N/A	10 ng/mL	46
4	Label-free immunosensor	10 μg/mL	7.5−25 μg/mL	5 h	N/A	47
5	FPOX/AuNPs/GO/CHIT/FTO	0.3 μM	0.1−2 mM	N/A	8.45 μA/mM/cm	48
6	WS_2-MIP/SPE electrochemical biosensor	0.01 pM	0.01pM-100 mM	10 min	0.27 μA/pM	Present work

repeatability with seven electrodes. The current difference was minimum within these electrodes. Hence, it can be concluded that the system is highly reproducible. The developed biosensor was compared with reported literature, as shown in Table 1. The present biosensor shows a lower limit of detection, wide concentration range, and fast incubation time.

4. CONCLUSION

In this present work, an electrochemical sensing platform was designed for easy and rapid detection of HbA1c. HbA1c is a specific biomarker for diabetes, and early detection will help in preventing severe conditions or disorders such as cardiovascular, retinopathy, neuropathy, and nephropathy. Presently, several methods are available for its detection, but they possess several limitations such as being time-consuming, expensive, cumbersome, and tedious. To overcome these constraints, this research work was carried out. The presented study is based on the imprinting technique integrated with nanomaterials. MIP was synthesized for the FAO enzyme, and this MIP was decorated with WS_2 NPs. The NPs enhance the electrical conductivity and analytical properties of the nanosensor. Further, the integration of synthesized MIP for FAO facilitates the high specificity of the biosensor. The platform was developed on an integrated electronic surface SPE. The surface of the working electrode was moderated using WS_2-MIP. Varying concentrations of HbA1c were used to evaluate the response of the designed biosensor. The concentration range for the fabricated biosensor was 0.01 pM to 100 mM, with a lower LOD (0.01 pM) and higher sensitivity of 0.27 μA/pM. The developed biosensor promises to produce early results; it is cost-effective, miniaturized in size, and can be easily converted into a portable device.

AUTHOR INFORMATION

Corresponding Author

Utkarsh Jain − *Amity Institute of Nanotechnology (AINT), Amity University Uttar Pradesh (AUUP), Noida 201313 Uttar Pradesh, India;* orcid.org/0000-0003-3901-0153; Phone: +91-7042663347; Email: ujain@amity.edu, karshjain@gmail.com

Authors

Sunil Kumar Mahobiya − *Amity Institute of Nanotechnology (AINT), Amity University Uttar Pradesh (AUUP), Noida 201313 Uttar Pradesh, India*

Sapna Balayan − *Amity Institute of Nanotechnology (AINT), Amity University Uttar Pradesh (AUUP), Noida 201313 Uttar Pradesh, India*

Nidhi Chauhan − *Amity Institute of Nanotechnology (AINT), Amity University Uttar Pradesh (AUUP), Noida 201313 Uttar Pradesh, India*

Manika Khanuja − *Centre for Nanoscience and Nanotechnology, Jamia Millia Islamia, New Delhi 110025, India*

Naresh K. Kuchhal − *Bio Diagnostic Laboratory, Delhi 110085, India*

S. S. Islam − *Centre for Nanoscience and Nanotechnology, Jamia Millia Islamia, New Delhi 110025, India;* orcid.org/0000-0001-7696-5499

Complete contact information is available at: https://pubs.acs.org/10.1021/acsomega.2c04926

Notes

The authors declare no competing financial interest.

REFERENCES

(1) Khalil, El. K.; El-Mernissi, R.; Hajji, H.; Singh, A. K.; Aziz, M. Identification of Novel Indole Derivatives as Potent α-Amylase Inhibitors for the Treatment of Type-II Diabetes Using in-Silico Approaches. *Biointerface Res. Appl. Chem.* **2022**, *13*, 76−92.

(2) American Diabetes Association. Diagnosis and classification of diabetes mellitus. *Proc. Am. Diabetes Assoc. Diabetes Care* 2010, *33*, S62−S69.

(3) World Health Organization. Use of glycated haemoglobin (HbA1c) in diagnosis of diabetes mellitus: abbreviated report of a WHO consultation. No. WHO/NMH/CHP/CPM/11.1; World Health Organization, 2011.

(4) Dubey, R.; Prabhakar, P. K.; Gupta, J. Identification of Structurally Similar Phytochemicals to Quercetin with High SIRT1 Binding Affinity and Improving Diabetic Wound Healing by Using In silico Approaches. *Biointerface Res. Appl. Chem.* **2021**, *12*, 7621−7632.

(5) Jain, U.; Soni, S.; Balhara, Y. P. S.; Khanuja, M.; Chauhan, N. Dual-layered nanomaterial-based molecular pattering on polymer surface biomimetic impedimetric sensing of a bliss molecule, anandamide neurotransmitter. *ACS omega* **2020**, *5*, 10750−10758.

(6) Belardja, M. S.; Djelad, H.; Lafjah, M.; Chouli, F.; Benyoucef, A. The influence of the addition of tungsten trioxide nanoparticle size on structure, thermal, and electroactivity properties of hybrid material−reinforced PANI. *Colloid Polym. Sci.* **2020**, *298* (11), 1455−1463.

(7) Samanta, S. Glycated hemoglobin and subsequent risk of microvascular and macrovascular complications. *Indian J. Med. Sci.* **2020**, *73* (2), 230−238.

(8) World Health Organization. *Global Report on Diabetes*; World Health Organization, 2016.

(9) Mahmood, J. S.; AL-Fatlawi, H. Y. Types of Diabetes and Their Effect on the Immune System. *J. Adv. Pharm. Prac.* **2022**, *4*, 21−30.

(10) Karimi-Maleh, H.; Beitollahi, H.; Senthil Kumar, P.; Tajik, S.; Mohammadzadeh Jahani, P.; Karimi, F.; Karaman, C.; Vasseghian, Y.; Baghayeri, M.; Rouhi, J.; Show, P. L.; Rajendran, S.; Fu, L.; Zare, N. Recent advances in carbon nanomaterials-based electrochemical sensors for food azo dyes detection. *Food Chem. Toxicol.* **2022**, *164*, 112961.

(11) Tajik, S.; Beitollahi, H. Hydrothermal synthesis of $CuFe_2O_4$ nanoparticles for highly sensitive electrochemical detection of sunset yellow. *Food Chem. Toxicol.* **2022**, *165*, 113048.

(12) Garkani Nejad, F.; Asadi, M. H.; Sheikhshoaie, I.; Dourandish, Z.; Zaimbashi, R.; Beitollahi, H. Construction of modified screen-

https://doi.org/10.1021/acsomega.2c04926
ACS Omega 2022, 7, 34676−34684

printed graphite electrode for the application in electrochemical detection of sunset yellow in food samples. *Food Chem. Toxicol.* **2022**, *166*, 113243.
(13) Tajik, S.; Lohrasbi-Nejad, A.; Mohammadzadeh Jahani, P.; Askari, M. B.; Salarizadeh, P.; Beitollahi, H. Co-detection of carmoisine and tartrazine by carbon paste electrode modified with ionic liquid and MoO_3/WO_3 nanocomposite. *J. of Food Meas. and Chara.* **2022**, *16*, 722−730.
(14) Tajik, S.; Orooji, Y.; Karimi, F.; Ghazanfari, Z.; Beitollahi, H.; Shokouhimehr, M.; Varma, R. S.; Jang, H. W. High performance of screen-printed graphite electrode modified with Ni−Mo-MOF for voltammetric determination of amaranth. *J. of Food Meas. and Chara.* **2021**, *15*, 4617−4622.
(15) Tajik, S.; Orooji, Y.; Ghazanfari, Z.; Karimi, F.; Beitollahi, H.; Varma, R. S.; Jang, H. W.; Shokouhimehr, M. Nanomaterials modified electrodes for electrochemical detection of Sudan I in food. *J. of Food Meas. and Chara.* **2021**, *15*, 3837−3852.
(16) Zhan, Z.; Li, Y.; Zhao, Y.; Zhang, H.; Wang, Z.; Fu, B.; Li, W. J. A Review of Electrochemical Sensors for the Detection of Glycated Hemoglobin. *Biosens.* **2022**, *12*, 221.
(17) Ahmadi, A.; Khoshfetrat, S. M.; Kabiri, S.; Dorraji, P. S.; Larijani, B.; Omidfar, K. Electrochemiluminescence paper-based screen-printed electrode for HbA1c detection using two-dimensional zirconium metal-organic framework/Fe_3O_4 nanosheet composites decorated with Au nanoclusters. *Microchim. Acta.* **2021**, *188*, 296.
(18) Pohanka, M. Glycated Hemoglobin and Methods for Its Point of Care Testing. *Biosens.* **2021**, *11*, 70.
(19) Reddy, K. K.; Bandal, H.; Satyanarayana, M.; Goud, K. Y.; Gobi, K. V.; Jayaramudu, T.; Amalraj, J.; Kim, H. Recent trends in electrochemical sensors for vital biomedical markers using hybrid nanostructured materials. *Adv. Sci.* **2020**, *7*, 1902980.
(20) Orooji, Y.; Asrami, P. N.; Beitollahi, H.; Tajik, S.; Alizadeh, M.; Salmanpour, S.; Baghayeri, M.; Rouhi, J.; Sanati, A. L.; Karimi, F. An electrochemical strategy for toxic ractopamine sensing in pork samples; twofold amplified nano-based structure analytical tool. *J. of Food Meas. and Chara.* **2021**, *15*, 4098−4104.
(21) Beitollahi, H.; Shahsavari, M.; Sheikhshoaie, I.; Tajik, S.; Jahani, P. M.; Mohammadi, S. Z.; Afshar, A. A. Amplified electrochemical sensor employing screen-printed electrode modified with Ni-ZIF-67 nanocomposite for high sensitive analysis of Sudan I in present bisphenol A. *Food Chem. Toxicol.* **2022**, *161*, 112824.
(22) Tajik, S.; Beitollahi, H.; Torkzadeh-Mahani, M. Electrochemical immunosensor for the detection of anti-thyroid peroxidase antibody by gold nanoparticles and ionic liquid-modified carbon paste electrode. *J. Nanostruct. Chem.* **2022**, *12*, 581−588.
(23) Jain, U.; Gupta, S.; Chauhan, N. Construction of an amperometric glycated hemoglobin biosensor based on Au−Pt bimetallic nanoparticles and poly (indole-5-carboxylic acid) modified Au electrode. *Int. J. Biol. Macromol.* **2017**, *105*, 549−555.
(24) Jain, U.; Gupta, S.; Chauhan, N. Detection of glycated hemoglobin with voltammetric sensing amplified by 3D-structured nanocomposites. *Int. J. Biol. Macromol.* **2017**, *101*, 896−903.
(25) Jain, U.; Chauhan, N. Glycated hemoglobin detection with electrochemical sensing amplified by gold nanoparticles embedded N-doped graphene nanosheet. *Biosens. Bioelectron.* **2017**, *89*, 578−584.
(26) Jain, U.; Singh, A.; Kuchhal, N. K.; Chauhan, N. Glycated hemoglobin biosensing integration formed on Au nanoparticle-dotted tubular TiO2 nanoarray. *Anal. Chim. Acta* **2016**, *945*, 67−74.
(27) Chauhan, N.; Jain, U. Influence of Zinc Oxide Nanorods on The Sensitivity of a Glycated Hemoglobin Biosensor. *Adv. Mater. Lett.* **2016**, *7*, 666−672.
(28) Bennett, C. M.; Guo, M.; Dharmage, S. C. HbA1c as a screening tool for detection of type 2 diabetes: a systematic review. *Diabetic Med.* **2007**, *24*, 333−343.
(29) Casadei, G.; Filippini, M.; Brognara, L. Glycated hemoglobin (HbA1c) as a biomarker for diabetic foot peripheral neuropathy. *Diseases* **2021**, *9*, 16.
(30) Chivese, T.; Hirst, J.; Matizanadzo, J. T.; Custodio, M.; Farmer, A.; Norris, S.; Levitt, N. The diagnostic accuracy of HbA1c, compared to the oral glucose tolerance test, for screening for type 2 diabetes mellitus in Africa—A systematic review and meta-analysis. *Diabetic Med.* **2022**, *39*, 14754.
(31) Quansah, D. Y.; Gross, J.; Mbundu-Ilunga, R.; Puder, J. J. The utility of diagnostic tests in the detection and prediction of glucose intolerance in the early and late postpartum period in women after gestational diabetes: a longitudinal cohort study. *Diabetol. Metab. Syndr.* **2021**, *13*, 31.
(32) Zhang, D.; Cao, Y.; Wu, J.; Zhang, X. Tungsten trioxide nanoparticles decorated tungsten disulfide nanoheterojunction for highly sensitive ethanol gas sensing application. *Appl. Surf. Sci.* **2020**, *503*, 144063.
(33) Liu, X.; Shuai, H. L.; Liu, Y. J.; Huang, K. J. An electrochemical biosensor for DNA detection based on tungsten disulfide/multi-walled carbon nanotube composites and hybridization chain reaction amplification. *Sens. Actuators, B* **2016**, *235*, 603−613.
(34) Gui, R.; Jin, H.; Guo, H.; Wang, Z. Recent advances and future prospects in molecularly imprinted polymers-based electrochemical biosensors. *Biosens. Bioelectron.* **2018**, *100*, 56−70.
(35) Uzun, L.; Turner, A. P. Molecularly-imprinted polymer sensors: Realising their potential. *Biosens. Bioelectron.* **2016**, *76*, 131−144.
(36) Cui, F.; Zhou, Z.; Zhou, H. S. Molecularly imprinted polymers and surface imprinted polymers based electrochemical biosensor for infectious diseases. *Sens.* **2020**, *20*, 996.
(37) Balayan, S.; Chauhan, N.; Chandra, R.; Jain, U. Electrochemical Based C-Reactive Protein (CRP) Sensing Through Molecularly Imprinted Polymer (MIP) Pore Structure Coupled with Bi-Metallic Tuned Screen-Printed Electrode. *Biointerface Res. Appl. Chem.* **2022**, *12*, 7697−7714.
(38) Balayan, S.; Chauhan, N.; Chandra, R.; Jain, U. Molecular imprinting based electrochemical biosensor for identification of serum amyloid A (SAA), a neonatal sepsis biomarker. *Int. J. Biol. Macromol.* **2022**, *195*, 589−597.
(39) Balayan, S.; Chauhan, N.; Kumar, P.; Chandra, R.; Jain, U. Fabrication of a sensing platform for identification of tumor necrosis factor-alpha: a biomarker for neonatal sepsis. *3 Biotech.* **2022**, *12*, 37.
(40) Jain, U.; Soni, S.; Balhara, Y. P. S.; Khanuja, M.; Chauhan, N. Dual-layered nanomaterial-based molecular pattering on polymer surface biomimetic impedimetric sensing of a bliss molecule, anandamide neurotransmitter. *ACS omega.* **2020**, *5*, 10750−10758.
(41) Dong, L.; Wang, Y.; Sun, J.; Pan, C.; Zhang, Q.; Gu, L.; Wan, B.; Song, C.; Pan, F.; Wang, C.; Tang, Z.; Zhang, J. Facile access to shape-controlled growth of WS2 monolayer via environment-friendly method. *2D Mater.* **2019**, *6*, 015007.
(42) Jain, U.; Chauhan, N. Glycated hemoglobin detection with electrochemical sensing amplified by gold nanoparticles embedded N-doped graphene nanosheet. *Biosens. Bioelectron.* **2017**, *89*, 578−584.
(43) Mahobiya, S. K.; Chauhan, N.; Balayan, S.; Kuchhal, N. K.; Islam, S. S.; Jain, U. Developing a Sensing Platform based on Molecular Imprinting of HbA1c on Fe3O4 Nanoparticle Modified Screen-Printed Electrode. *Biointerface Res. Appl. Chem.* **2022**, *13*, 228−240.
(44) Eissa, S.; Zourob, M. Aptamer-based label-free electrochemical biosensor array for the detection of total and glycated hemoglobin in human whole blood. *Sci. Rep.* **2017**, *7*, 1016.
(45) Zhang, C. G.; Chang, S. J.; Settu, K.; Jung Chen, C.; Liu, J. T. High-sensitivity glycated hemoglobin (HbA1c) aptasensor in rapid-prototyping surface plasmon resonance. *Sens. Actuators, B* **2019**, *279*, 267−273.
(46) Ahn, K. S.; Lee, J. H.; Park, J. M.; Choi, H. N.; Lee, W. Y. Luminol chemiluminescence biosensor for glycated hemoglobin (HbA1c) in human blood samples. *Biosens. Bioelectron.* **2016**, *75*, 82−87.
(47) Molazemhosseini, A.; Magagnin, L.; Vena, P.; Liu, C. C. Single-use disposable electrochemical label-free immunosensor for detection of glycated hemoglobin (HbA1c) using differential pulse voltammetry (DPV). *Sens.* **2016**, *16*, 1024.
(48) Shahbazmohammadi, H.; Sardari, S.; Omidinia, E. An amperometric biosensor for specific detection of glycated hemoglobin

https://doi.org/10.1021/acsomega.2c04926
ACS Omega 2022, 7, 34676−34684

based on recombinant engineered fructosyl peptide oxidase. *Int. J. Biol. Macromol.* **2020**, *142*, 855−865.

https://doi.org/10.1021/acsomega.2c04926
ACS Omega 2022, 7, 34676−34684